Distinct Bioenergetic Features of Human Invariant Natural Killer T Cells Enable Retained Functions in Nutrient-Deprived States

Priya Khurana[1,2], Chakkapong Burudpakdee[1], Stephan A. Grupp[2,3], Ulf H. Beier[2,4,5], David M. Barrett[6] and Hamid Bassiri[1,2*]

[1] Division of Infectious Diseases, Department of Pediatrics, Children's Hospital of Philadelphia, Philadelphia, PA, United States, [2] Perelman School of Medicine, University of Pennsylvania, Philadelphia, PA, United States, [3] Cell and Therapy Transplant Section, Division of Oncology, Children's Hospital of Philadelphia, Philadelphia, PA, United States, [4] Division of Nephrology, Department of Pediatrics, Children's Hospital of Philadelphia, Philadelphia, PA, United States, [5] Janssen Research and Development, Spring House, PA, United States, [6] Tmunity Therapeutics, Philadelphia, PA, United States

Invariant natural killer T (iNKT) cells comprise a unique subset of lymphocytes that are primed for activation and possess innate NK-like functional features. Currently, iNKT cell-based immunotherapies remain in early clinical stages, and little is known about the ability of these cells to survive and retain effector functions within the solid tumor microenvironment (TME) long-term. In conventional T cells (T_{CONV}), cellular metabolism is linked to effector functions and their ability to adapt to the nutrient-poor TME. In contrast, the bioenergetic requirements of iNKT cells – particularly those of human iNKT cells – at baseline and upon stimulation are not well understood; neither is how these requirements affect effector functions such as production of cytokines and cytolytic proteins. We find that unlike T_{CONV}, human iNKT cells are not dependent upon glucose or glutamine for these effector functions upon stimulation with anti-CD3 and anti-CD28. Additionally, transcriptional profiling revealed that stimulated human iNKT cells are less glycolytic than T_{CONV} and display higher expression of fatty acid oxidation (FAO) and adenosine monophosphate-activated protein kinase (AMPK) pathway genes. Furthermore, stimulated iNKT cells displayed higher mitochondrial mass and membrane potential relative to T_{CONV}. Real-time Seahorse metabolic flux analysis revealed that stimulated human iNKT cells utilize fatty acids as substrates for oxidation more than stimulated T_{CONV}. Together, our data suggest that human iNKT cells possess different bioenergetic requirements from T_{CONV} and display a more oxidative metabolic program relative to effector T_{CONV}. Importantly, iNKT cell-based immunotherapeutic strategies could co-opt such unique features of iNKT cells to improve their efficacy and longevity of anti-tumor responses.

Keywords: immunometabolism, glycolysis, cytokine production and cytotoxicity, fatty acid oxidation (FAO), human invariant natural killer T cells (iNKT) cells

INTRODUCTION

Invariant natural killer T (iNKT) cells comprise a subset of innate-like T lymphocytes with TCR specificity for glycolipid antigens presented by the monomorphic, MHC I-like molecule CD1d (1). iNKT cells possess innate-like effector cell features, including rapid activation, cytokine secretion, and trafficking to tumor sites; as such, iNKT cells bridge innate and adaptive immune responses (2, 3). The presence of both circulating and intratumoral iNKT cells predicts more favorable tumor prognosis and survival in patients with several solid and liquid tumors [reviewed in (4)], suggesting that these cells play central roles in cancer immunity. This notion is supported by a body of literature [reviewed in (5)] that demonstrate that iNKT cells engage in both direct anti-tumor cytotoxicity against CD1d-expressing tumors (6, 7) and modulate the activity of many other immune cells, including natural killer (NK) cells, CD8$^+$ T cells (8–13), and myeloid cells (14–16).

Recently, iNKT cells have begun to be utilized as a platform for cellular immunotherapy, as adoptively-transferred cells (17–19) and chimeric antigen receptor (CAR)-transduced effectors directed against tumor antigens in lymphoma and solid tumor models (20, 21). While the studies published to date have demonstrated some efficacy, these trials are in early clinical stages and very little is understood about the basic cellular properties of iNKT cells that govern their ability to adapt to the tumor microenvironment (TME). Thus, in order to better inform the design of iNKT cell-based solid tumor immunotherapies in the future, there is a great need to better understand the metabolic properties of iNKT cells and how these are linked to anti-tumor effector functions.

In T_{CONV}, cellular metabolism is tightly linked to effector functions. Naïve T cells, which are relatively quiescent, predominantly utilize oxidative phosphorylation (OXPHOS) to maintain basal homeostasis and survival. Upon TCR stimulation, T_{CONV} undergo metabolic reprogramming as they differentiate into effector cells, whereby they preferentially rely on glycolysis and glutaminolysis to fuel substrate biogenesis and effector functions (22). Memory T cells predominantly utilize fatty acid oxidation (FAO) metabolism which enables greater survival and persistence within nutrient-poor environments; upon re-activation, memory T cells also shift to glycolytic metabolism as they differentiate into effector cells (23). In the TME, the long-term functional capacity of T_{CONV} is minimized as they compete with tumor cells and tumor-supporting myeloid cells for limited glucose and glutamine (24, 25). In contrast, memory T cells are more persistent within the TME (26–28). In addition, regulatory T cells (T_{REG}) rely on OXPHOS and FAO (29), allowing them to maintain immunosuppressive functions within the TME. Given that the metabolic profiles of T_{CONV} and other immune cells have been demonstrated to directly influence tumor progression, the use of therapies that modulate TME metabolism represent attractive treatment options for solid tumors.

In contrast to T_{CONV}, however, little is known about iNKT cell metabolism and its link to key anti-tumor effector functions such as cytokine production and cytotoxicity. Unlike T_{CONV}, iNKT cells do not have distinct differentiation states and exit the thymus primed for activation (30); these functional differences may indicate a unique underlying metabolic phenotype. Indeed, murine iNKT cells have been demonstrated to depend predominantly on OXPHOS for survival (31) and have also been shown to increase lipid biosynthesis upon activation, both *in vitro* and within the TME (32). Together, these data suggest that murine iNKT cells may have different bioenergetic profiles from T_{CONV}, which could have significant consequences for their survival and function within the TME. While these studies have begun to elucidate the metabolic profiles of murine iNKT cells, a metabolic characterization of human peripheral blood iNKT cells and how it is linked to effector functions relative to T_{CONV} has not been determined previously. Importantly, an understanding of human iNKT cell immunometabolism could have particular translational value for our ability to utilize these cells therapeutically, and is therefore a major gap in the field.

In the present study, we sought to delineate the metabolic and functional properties of rested and stimulated human iNKT cells relative to T_{CONV} under both normal and nutrient-deplete conditions. Using peripheral blood-derived iNKT cells and matched T_{CONV} from healthy human donors, we demonstrate distinct bioenergetic requirements between iNKT cells and T_{CONV} for the production of cytokines and cytolytic proteins after TCR stimulation. Specifically, we demonstrate that iNKT cells maintain effector functions in glucose- and glutamine-depleted conditions, and furthermore, utilize FAO metabolism to a greater extent than do T_{CONV}. Our findings not only unveil novel bioenergetic features of primary human iNKT cells, but also suggest that iNKT cells possess metabolic properties that may confer differential functional features and adaptability and longevity to the nutrient-poor TME. Importantly, these features could be co-opted in the design of future iNKT cell-based solid tumor immunotherapies.

MATERIALS AND METHODS

Human Primary Immune Cell Purification

Healthy, de-identified human donor peripheral mononuclear blood cells (PBMC) and conventional T cells (T_{CONV}) were purchased from the University of Pennsylvania Human Immunology Core under an institutional review board-approved protocol. To obtain sufficient yields of invariant natural killer (iNKT) cells, PBMC were plated in AIM V media (Gibco) containing 500ng/mL alpha-galactosylceramide (Cayman Chemicals; KRN7000) and 50U/mL recombinant IL-2 (PeproTech); on day 3-4 of culture, cells were fed with 10ng/mL recombinant IL-15 (BioLegend) and 10U/mL IL-2. On days 7-8 of expansion, iNKT cells were FACS-sorted from expanded PBMC (Vα24$^+$ CD3$^+$ cells) on BD Aria II or Aria Fusion instruments housed at the University of Pennsylvania and the Children's Hospital of Philadelphia Flow Cytometry Core Facilities, respectively. In parallel, CD4$^+$ and CD8$^+$ T cells were purified from whole blood using Rosette Sep negative selection kits (Stem Cell Technologies, cat# 15062 and #15063) by the Penn Human Immunology Core, per manufacturer's

instructions. T cells obtained from matched donors to corresponding PBMC were mixed at a 1:1 ratio to ensure equal composition of T_{CONV} populations.

Cell Culture and Stimulation of Purified Lymphocytes

Purified iNKT and pooled T_{CONV} (1:1 CD4$^+$:CD8$^+$) populations were subject to either "rest" (low dose 30U/mL IL-2 only) or stimulation using Dynabeads Human T-Expander CD3/28 (ThermoFisher Scientific) at 1 million cells/mL at a ratio of 2 beads per cell for 48 hours. For all studies of rested and stimulated cells under normal conditions (transcriptional profiling and flow-based dyes), cells were cultured in AIM V media containing 10% FBS and 1% L-glutamine. For glucose deprivation studies, cells were rested and stimulated in complete RPMI 1640 media (Gibco) containing 10% dialyzed FBS and 1% L-glutamine supplemented with either 10mM glucose, 1mM glucose, or 0.1mM glucose (Corning). For glutamine deprivation studies, cells were plated in either complete RPMI media (containing 10% FBS and 1% L-glutamine at an approximate concentration of 4mM glutamine total), or glutamine-free RPMI (Gibco) containing 10% dialyzed FBS supplemented with 10mM glucose. For inhibition of glucose metabolism, 2-deoxy-D-glucose (Sigma cat # D6134) was added to cells at concentrations of 2mM or 20mM for 48 hours. For all RNA (qPCR, NanoString) and cytokine profiling (ELISA, MSD) studies, harvested RNA and supernatants from rested and stimulated iNKT cells and T_{CONV} were banked at 48 hours and run and analyzed simultaneously.

Flow Cytometry

To sort iNKT cells, the following antibodies were used for staining: anti-Vα24-Jα18 (clone 6B11; BioLegend #342912), anti-CD3 (clone OKT3; BioLegend #317318). For staining of purified lymphocyte populations, cells were first stained with Zombie Aqua fixable live/dead exclusion dye per manufacturer's instructions (BioLegend cat #423101), followed by surface staining in FACS buffer containing 2.5% FBS. For intracellular staining, cells were fixed and permeabilized using the Becton Dickinson Cytofix/Cytoperm kit, according to manufacturer's instructions (BD Biosciences cat #554714) and stained with antibodies against granzyme B (clone QA16A02; BioLegend #372208) or mouse IgG1k isotype control (clone MOPC-21; BD Biosciences cat #556650), or Cpt1a (clone8F6AE9; Abcam cat# 171449) and rabbit IgG monoclonal isotype control (clone EPR25A; Abcam cat# 199091). For all flow cytometry studies, rested and stimulated iNKT cells and T_{CONV} were run on the same in-house instrument [FACSVerse cytometer (BD Biosciences)] on different days, and normalized to isotype controls within each sample, in order to minimize day-to-day variations. Mean fluorescent intensity (MFI) values of intracellular proteins (granzyme B and Cpt1a) were calculated by subtracting the isotype control MFI in each sample. Flow cytometry analysis was conducted using FlowJo software (Tree Star Inc.).

Mitochondrial Dye Staining

Purified rested and stimulated human iNKT cells and T_{CONV} were harvested at 48 hours for staining in either 200nM MitoTracker Green (Invitrogen cat #M7514) or 20nM tetramethylrhodamine, methyl ester (TMRM; Invitrogen cat #T668) in serum-free RPMI media for 45 minutes at 37°C per manufacturer's protocol.

RNA Purification and Quantitative Real-Time PCR

Total RNA was isolated from rested and stimulated iNKT cells and T_{CONV} using miRNeasy Mini kit per manufacturer's protocol (Qiagen). RNA was either hybridized for NanoString transcriptional analysis or converted to cDNA for qPCR analysis. For gene expression analysis of *Ifng*, cDNA was synthesized from purified mRNA using High Capacity Reverse Transcriptase kit (Applied Biosystems) according to manufacturer's protocol. Quantitative real-time PCR was performed on 7900HT Fast Real-Time PCR system (Applied Biosystems). Relative gene expression was calculated by normalizing delta Ct values for each target probe to *Actb* levels for each sample using the $2^{-\Delta Ct}$ method. The following TaqMan Gene Expression Assays (Life Technologies) were used: human *Ifng* (Hs_00989291_m1), human *Actb* (Hs01060665_g1).

NanoString nCounter Gene Expression Profiling and Analysis

Transcriptional profiling of mRNA isolated from rested and stimulated human iNKT cells and T_{CONV} was performed using the nCounter SPRINT Profiler (NanoString Technologies). Briefly, per manufacturer's instructions, 50ng of each RNA sample was hybridized for 18 hours at 65°C with reporter and capture probe sets for the Human Metabolic Pathways panel (containing 768 genes across several annotated metabolic pathways and 20 internal reference genes). Hybridized RNA samples were then loaded onto nCounter SPRINT cartridge to run on SPRINT Profiler instrument. Gene expression analysis was conducted using NanoString nSolver 4.0 software. Genes with counts under 100 were eliminated from analysis. Heatmaps were generated using Morpheus (https://software.broadinstitute.org/morpheus).

Cytokine Analysis

Supernatants from 48-hour rested and stimulated iNKT cells and T_{CONV} were assayed for cytokine levels of IFN-γ using human ELISA kit (Invitrogen cat #88-7316) following manufacturer's protocol. Quantification of TNF-α and IL-4 cytokines in supernatants was performed using V-Plex Pro-Inflammatory Panel 1 Human Kit (Meso Scale Discovery, cat #K15049D). Assays were performed per manufacturer's protocol and read and analyzed on a Meso Scale Discovery QuickPlex SQ120 instrument.

Seahorse XF Metabolic Analysis

Real-time metabolic measurements of oxygen consumption rate (OCR) and extracellular acidification rate (ECAR) of iNKT cells

and T_{CONV} from matched donors were obtained using XFe96 Extracellular Flux Analyzer (Seahorse Biosciences). On the day prior to assay, XF cartridge was hydrated, and XF tissue microplates were coated with Cell Tak (Corning cat #354240) per manufacturer's protocol. On the day of the assay, 48-hour stimulated iNKT cells and T_{CONV} were washed and seeded at a density of 220,000 cells per well on pre-coated tissue microplates in XF RPMI assay media (pH 7.4) supplemented with 10mM glucose, 2mM L-glutamine, and 1mM pyruvate. Cells were spun down at 1500rpm for 3 minutes to facilitate adherence and placed in non-CO_2 incubator for one hour prior to running assay. The Long-Chain Fatty Acid Substrate Oxidation kit (Agilent cat #103672-100) was utilized to probe differences in OCR upon injection with either vehicle (media only) or etomoxir (4μM) to inhibit long-chain fatty acid oxidation. Following three basal measurements of OCR and ECAR, cells were sequentially injected with 1.5μM oligomycin A (ATP synthase inhibitor; Agilent Technologies), 0.5μM FCCP (mitochondrial uncoupling agent; Agilent Technologies), and 0.5μM rotenone/antimycin A (mitochondrial complex I and III inhibitors; Agilent Technologies). After injection of oligomycin A, six readings were taken; after the following two sequential injections, three readings were taken. Maximal respiration was calculated as the difference between OCR upon FCCP injection and non-mitochondrial respiration (OCR upon rotenone and antimycin A injection). ATP production was calculated as the difference in OCR prior to and after oligomycin A injection.

Statistical Analyses

For comparison of relative fold-changes in mRNA, ELISA, and Seahorse assays, unpaired student's t-tests were utilized to assess significance between groups. For flow cytometry data assessing mean fluorescent intensity values in iNKT cells and T_{CONV} (e.g. granzyme B, Cpt1a, MitoTracker, and TMRM), two-way analysis of variance (ANOVA) analyses were performed. To assess dose-dependence of glucose concentration on mean fluorescent values of stimulated iNKT cells and T_{CONV}, simple linear regression was conducted. As denoted in the figure legends, significance was indicated by $p<0.05$ (*), $p<0.01$ (**), and $p<0.001$ (***). All graphs and statistical analyses were conducted using GraphPad Prism software.

RESULTS

Human iNKT Cells Maintain Effector Functions in Glucose-Depleted Culture Conditions Relative to T_{CONV}

To reliably obtain sufficient numbers of iNKT cells for our studies, we used populations of expanded, de-identified healthy human donor peripheral blood mononuclear cells (PBMC) and purified conventional T cells (T_{CONV}) from matched donors (as per the schematic in **Supplementary Figure 1**). Given the well-documented metabolic profiles of T_{CONV} upon TCR stimulation, we opted to use these cells as positive and negative controls, by which to compare iNKT cell metabolism in our metabolic and

functional assays. Thus, we utilized an equal ratio of $CD4^+$ and $CD8^+$ cells to ensure uniformity across experiments. To compare the metabolic and functional properties of human iNKT cells relative to matched T_{CONV} under identical conditions, each cell type was subjected to 48 hours of either rest (low-dose IL-2 only) or stimulation using anti-CD3/anti-CD28-coated microbeads.

We first investigated the dependency of human iNKT cells on glucose for anti-tumor cytokine production and cytotoxicity. Glucose is a limited nutrient within the TME and is rapidly metabolized by highly glycolytic tumor cells. Indeed, several prior studies have demonstrated that *in vitro* glucose depletion impairs the effector functions of T_{CONV} (33–35) and that reliance on glycolysis confers poorer persistence and survival within the TME (27, 36). A recent study suggested that mouse iNKT cells uptake less glucose than $CD4^+$ T cells (31), suggesting that they may be less reliant on glucose metabolism. To assess the requirement of glucose for human iNKT cell effector functions, iNKT cells and T_{CONV} were rested or stimulated in culture conditions containing either standard glucose (10mM) or depleted glucose (1mM or 0.1mM) concentrations for 48 hours. Intriguingly, iNKT cells were able to maintain levels of both *Ifng* mRNA and secreted IFN-γ upon stimulation in low glucose media (**Figures 1A–D**). In contrast, T_{CONV} were sensitive to glucose depletion and demonstrated a dose-dependent decrease in *Ifng* transcripts and IFN-γ secreted protein levels. Strikingly, in 0.1mM glucose conditions, T_{CONV} displayed an 85% reduction in stimulation-induced *Ifng* mRNA and an over 70% reduction in IFN-γ protein secretion relative to 10mM glucose, while iNKT cells had no significant changes in IFN-γ levels (**Figures 1A–D**). In addition to IFN-γ secretion, we also observed similar results in the secretion of additional cytokines, including TNF-α and IL-4 (**Supplementary Figures 2A, B**), whereby iNKT cells did not rely on glucose for stimulation-induced secretion of these cytokines while T_{CONV} demonstrated dose-dependent decreases in TNF-α and IL-4 secretion with lower glucose.

We next investigated the dependency of these cells on glucose for cytotoxicity by measuring levels of intracellular granzyme B, a cytolytic protein we have utilized to infer cytotoxic effector function. We found that stimulated iNKT cells maintain similar levels of intracellular granzyme B in glucose-deplete conditions, whereas T_{CONV} consistently displayed a significant, dose-dependent reduction in granzyme B levels upon stimulation in lowered glucose concentrations (**Figure 1E**). Indeed, in 0.1mM glucose conditions, stimulated T_{CONV} granzyme B levels were reduced by approximately 85% relative to 10mM glucose, while stimulated iNKT cells displayed no significant differences in granzyme B with reduced glucose (**Figure 1F**). As an additional approach, we also treated iNKT cells and T_{CONV} with 2-deoxy-D-glucose (2-DG), a synthetic glucose analog that inhibits downstream glucose metabolism (37). Although at a higher concentration of 2-DG (20mM), the effector functions of both iNKT cells and T_{CONV} were impaired, with a lower dose of 2-DG (2mM), iNKT cell cytokine production and granzyme B production were not significantly different relative to untreated conditions, whereas T_{CONV}
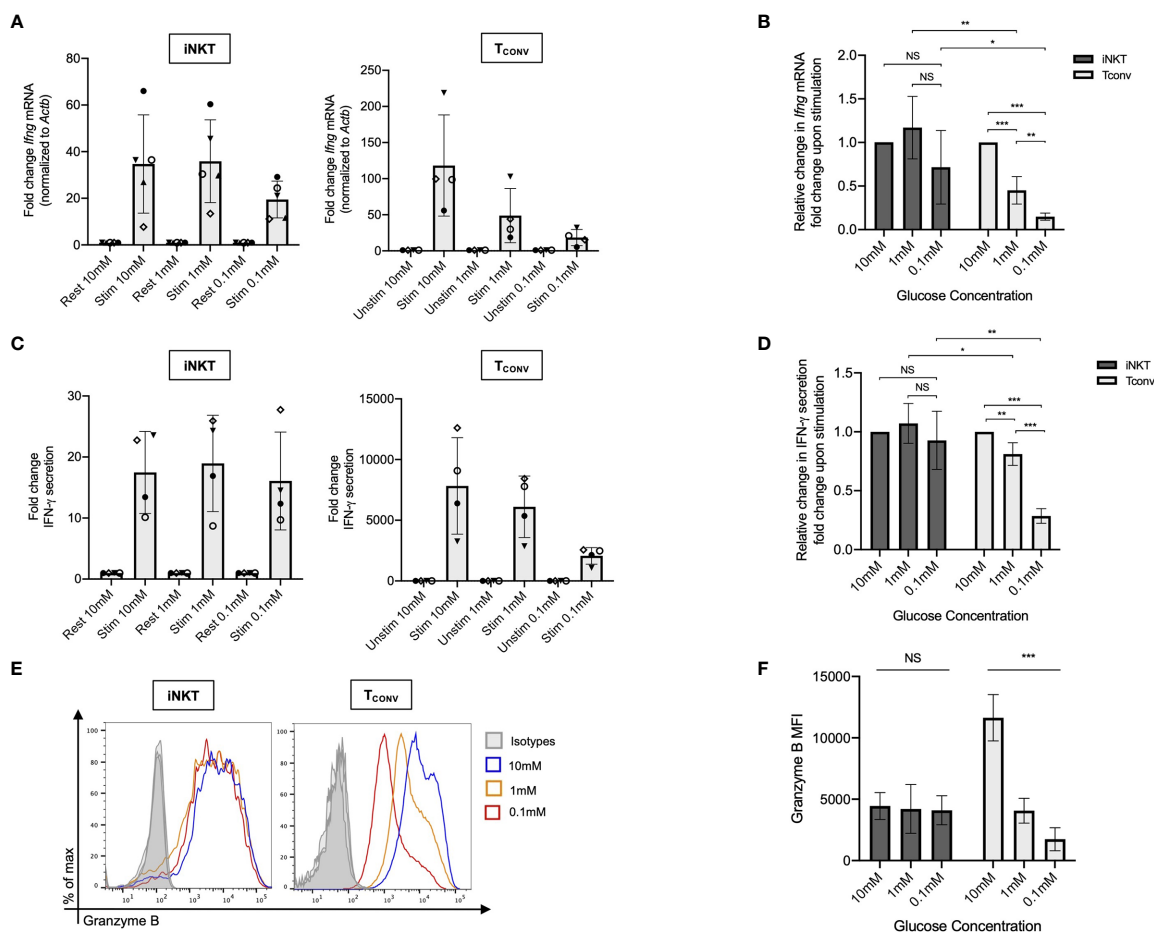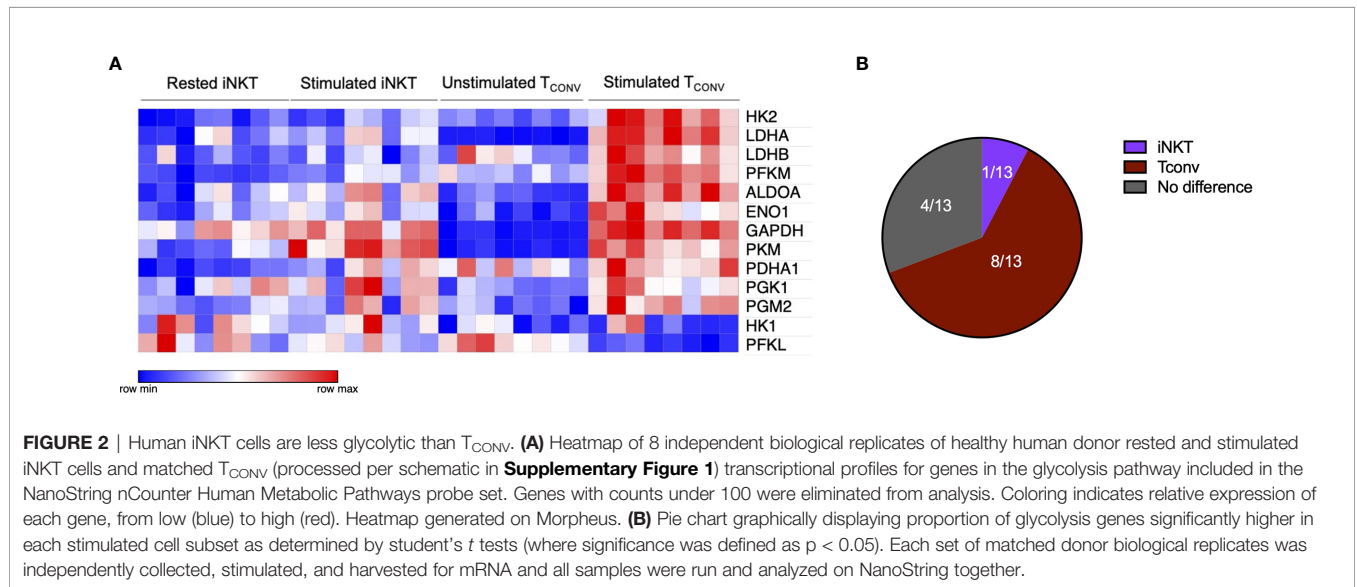
FIGURE 1 | Human iNKT cells do not depend on glucose for effector functions relative to T_{CONV}. Sorted PBMC-derived iNKT cells and T_{CONV} were rested or stimulated in RPMI media containing 10mM, 1mM, or 0.1mM glucose for 48 hours per schematic in **Supplementary Figure 1**. **(A)** mRNA expression of *Ifng* was determined for iNKT cells (left) and T_{CONV} (right) at 48 hours by qPCR (with values normalized to *Actb* expression). Fold change induction of *Ifng* upon stimulation relative to rest (iNKT) and unstimulated (T_{CONV}) conditions displayed. Each symbol represents matched, independent human donor biological replicates. **(B)** Summary data depicting fold change in *Ifng* Ct values upon stimulation from qPCR in **(A)**, relative to 10mM glucose, for iNKT and T_{CONV} **(C)** Supernatants were collected from rested and stimulated iNKT cells (left) and T_{CONV} (right) after 48 hours. IFN-γ levels were detected *via* ELISA and fold change upregulation upon stimulation relative to rest (iNKT) and unstimulated (T_{CONV}) conditions displayed. Each symbol represents matched, independent human donor biological replicates. **(D)** Summary data depicting fold change in IFN-γ secretion upon stimulation from ELISA in **(C)**, relative to 10mM glucose, for iNKT and T_{CONV}. **(E)** Rested and stimulated iNKT cells and T_{CONV} from matched human donors were stained for intracellular Granzyme B or isotype control; histogram of live, stimulated iNKT cells and T_{CONV} representative of 4 matched, independent human donor samples. **(F)** Quantification of granzyme B mean fluorescence intensity (MFI) of stimulated iNKT cells and T_{CONV} normalized to isotype MFI indicated in bar graph. In all graphs, asterisks denote statistical significance (NS, non-significant; *$p < 0.05$, **$p < 0.01$, ***$p < 0.001$) determined by unpaired, two-way student's *t* tests in **(B, D)** and simple linear regression test in **(F)**. For all studies, biological replicates of human donor samples are indicated by symbols, and n=4 technical replicates were performed. Each biological replicate of matched donor cells was run in independent experiments.

maintained sensitive to glycolytic inhibition (**Supplemental Figures 3A–C**). Collectively, these data further support the notion that iNKT cells are less glucose-dependent for effector functions than T_{CONV} and likely utilize alternate metabolic pathways upon stimulation.

Human iNKT Cells Are Less Glycolytic Than T_{CONV}

The striking differences in the sensitivity of iNKT cells and T_{CONV} to glucose depletion suggest a potential underlying difference in glycolytic metabolism. While T_{CONV} upregulate

glycolysis upon stimulation, the metabolic activity of human iNKT cells is unknown. Using a NanoString probe set with over 700 curated transcripts for genes involved in cancer immunology and metabolism, we assayed changes in the mRNA expression of metabolic genes in rested and stimulated PBMC-derived iNKT cells and matched T_{CONV} from 8 independent donors. In contrast to T_{CONV}, which upregulated glycolytic pathway enzyme transcripts upon stimulation, iNKT cells only upregulated a small subset of the glycolytic genes upon stimulation, and to a lesser extent than T_{CONV} (**Figure 2A**). Indeed, of the 13 glycolytic genes probed, 9 were significantly

FIGURE 2 | Human iNKT cells are less glycolytic than T_{CONV}. **(A)** Heatmap of 8 independent biological replicates of healthy human donor rested and stimulated iNKT cells and matched T_{CONV} (processed per schematic in **Supplementary Figure 1**) transcriptional profiles for genes in the glycolysis pathway included in the NanoString nCounter Human Metabolic Pathways probe set. Genes with counts under 100 were eliminated from analysis. Coloring indicates relative expression of each gene, from low (blue) to high (red). Heatmap generated on Morpheus. **(B)** Pie chart graphically displaying proportion of glycolysis genes significantly higher in each stimulated cell subset as determined by student's t tests (where significance was defined as $p < 0.05$). Each set of matched donor biological replicates was independently collected, stimulated, and harvested for mRNA and all samples were run and analyzed on NanoString together.

differentially expressed between stimulated T_{CONV} and stimulated iNKT cells, and of these 9 genes, 8 were significantly higher in T_{CONV}: *Pfkm, Hk2, Ldha, Ldhb, Aldoa, Eno1, Gapdh*, and *Pdha1* (**Figure 2B** and **Table 1**). Each of these genes encode key enzymes throughout the glycolysis pathway that also fuel additional biosynthetic pathways.

In T_{CONV}, the transcription factor Myc is a master regulator required for initiation and maintenance of glycolytic metabolic reprogramming after TCR stimulation (38). In iNKT cells, the role of Myc, particularly upon activation, has not been previously examined. Consistent with reduced glycolytic reprogramming in stimulated iNKT cells, we also found that iNKT cells have significantly lower upregulation of Myc pathway genes than stimulated T_{CONV} (**Supplementary Figures 4A, B** and **Supplementary Table 1**). This difference in transcription of genes downstream of Myc signaling could suggest a mechanistic difference in the metabolic regulation of these two cell types.

Together, both the glycolysis and Myc pathway gene expression data suggest that human iNKT cells, in comparison

to T_{CONV}, employ distinct metabolic pathways from T_{CONV} upon TCR stimulation. Importantly, iNKT cells' lack of dependence on glycolysis could be advantageous in the context of the TME, whereby iNKT cells may be able to maintain certain effector functions in glucose-diminished conditions in which T_{CONV} are at a disadvantage.

Human iNKT Cells Are Less Sensitive to Glutamine Depletion Than T_{CONV} for Maintaining Effector Functions

Given that stimulated human iNKT cells were not dependent on glucose metabolism for effector functions, we wondered if they instead utilize glutamine as an alternative metabolic substrate to fuel cytokine production and cytotoxicity. Through glutaminolysis, glutamine is metabolized into α-ketoglutarate, which directly enters the TCA cycle to eventually yield ATP *via* oxidative phosphorylation (OXPHOS). Upon TCR activation, T_{CONV} increase both glutamine and glucose uptake and metabolism in order to fuel effector functions (38–40). In contrast, the role of glutamine has not yet been elucidated in

TABLE 1 | Glycolysis pathway gene set expression in stimulated iNKT cells and T_{CONV}.

Gene name	p-value	q-value	Higher expressing cell subset
PFKL	1.8003E-05	1.6498E-04	iNKT
PFKM	2.7224E-05	1.6498E-04	T_{CONV}
HK2	7.0098E-05	2.8319E-04	T_{CONV}
LDHA	1.2875E-04	3.9011E-04	T_{CONV}
LDHB	2.0950E-04	4.2319E-04	T_{CONV}
ALDOA	6.6621E-03	1.0093E-02	T_{CONV}
ENO1	1.8666E-02	2.1844E-02	T_{CONV}
GAPDH	1.9826E-02	2.1844E-02	T_{CONV}
PDHA1	2.7659E-02	2.7936E-02	T_{CONV}
PGM2	7.5981E-02	6.5778E-02	T_{CONV}
HK1	1.2941E-01	1.0457E-01	iNKT
PKM	2.0838E-01	1.5785E-01	iNKT
PGK1	9.5339E-01	6.0816E-01	iNKT

iNKT cells. To investigate whether glutamine is required for iNKT cell effector functions, we rested and stimulated matched human iNKT and T_{CONV} in either complete or glutamine-free media using the schema described in **Supplementary Figure 1**. Upon stimulation in glutamine-deplete conditions, iNKT cells display a slight but non-significant decrease in *Ifng* mRNA expression of approximately 40% relative to those stimulated in complete media, whereas T_{CONV} reduced stimulation-induced *Ifng* mRNA expression by ~60% in glutamine-free conditions relative to complete media (**Figures 3A, B**). Strikingly, IFN-γ secretion was not altered in iNKT cells stimulated in the absence

of glutamine, whereas it was reduced by ~90% in T_{CONV} (**Figures 3C, D**). These data imply a differential reliance on glutamine for cytokine production between these cell types. Additionally, iNKT cells secreted similar levels of TNF-α and IL-4 cytokines when stimulated in glutamine-deplete conditions relative to complete media (**Supplementary Figures 5A, B**). Furthermore, while glutamine depletion almost entirely abrogated T_{CONV} intracellular granzyme B levels, iNKT cells were able to retain some granzyme B production even when stimulated in the absence of glutamine – measuring ~65% of that of levels in normal conditions (**Figures 3E, F**). Thus, this
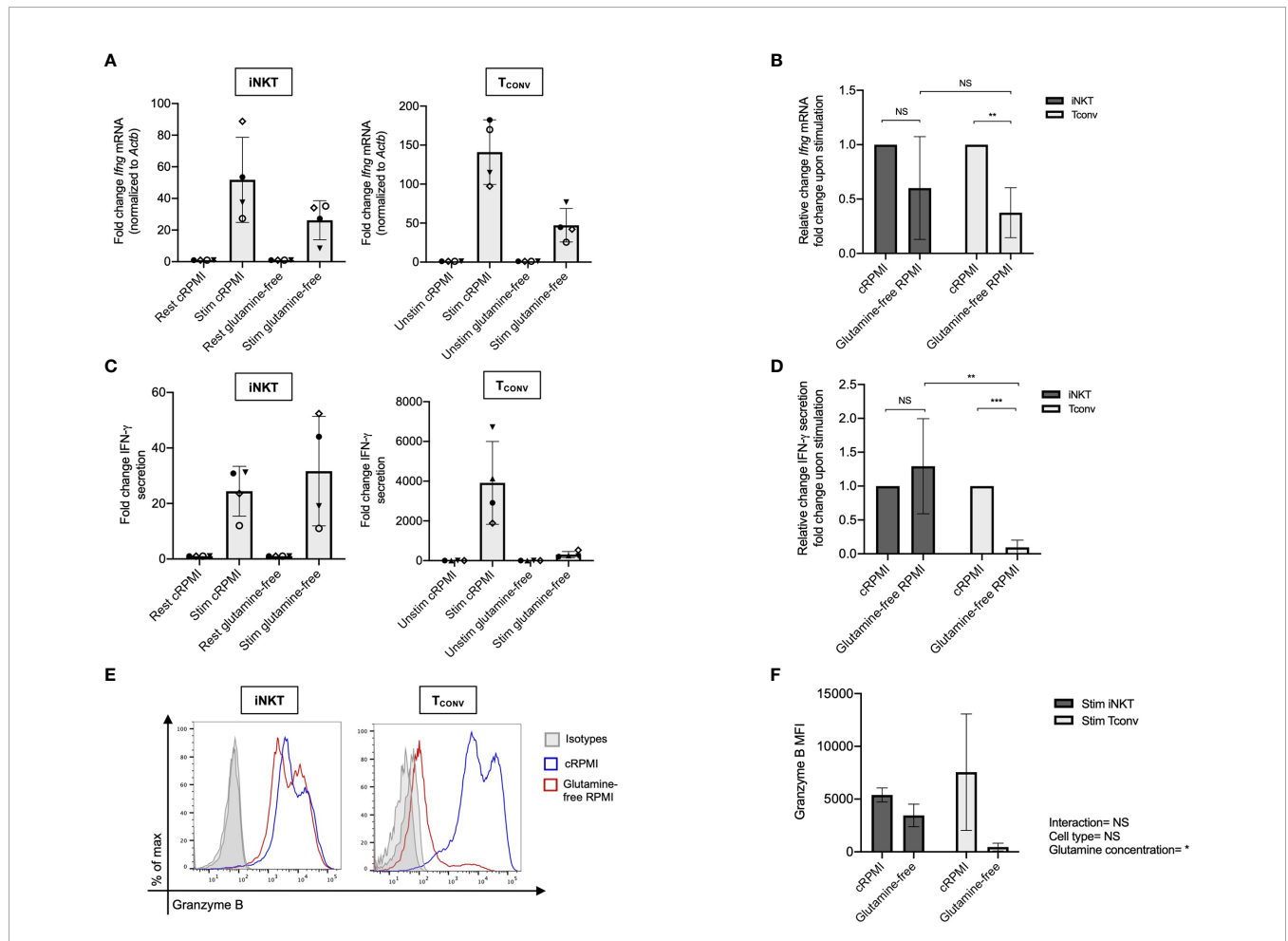

FIGURE 3 | Human iNKT cells are less reliant on glutamine for effector functions than T_{CONV}. Sorted PBMC-derived iNKT cells and T_{CONV} were rested or stimulated in either complete RPMI (10% FBS, 1% L-glutamine) or glutamine-free RPMI media for 48 hours per schematic in **Supplementary Figure 1**. **(A)** mRNA expression of *Ifng* was determined for iNKT cells (left) and T_{CONV} (right) at 48 hours by qPCR (with values normalized to *Actb* expression). Fold change induction of *Ifng* upon stimulation relative to rest (iNKT) and unstimulated (T_{CONV}) conditions displayed. Each symbol represents matched, independent human donor biological replicates. **(B)** Summary data of fold change in *Ifng* Ct upon stimulation relative to cRPMI condition is depicted for iNKT and T_{CONV} from qPCR in **(A)**. **(C)** Supernatants were collected from rested and stimulated iNKT cells (left) and T_{CONV} (right) after 48 hours. IFN-γ levels were detected *via* ELISA and fold change upregulation upon stimulation relative to rest (iNKT) and unstimulated (T_{CONV}) conditions displayed. Each symbol represents matched, independent human donor replicates. **(D)** Summary data of change in IFN-γ secretion fold change upon stimulation relative to cRPMI is depicted for iNKT and T_{CONV} from ELISA in **(C)**. **(E)** Rested and stimulated iNKT cells and T_{CONV} from matched human donors were stained for intracellular Granzyme B or isotype control; histogram of live, stimulated iNKT cells and T_{CONV} representative of 4 matched, independent human donor samples. **(F)** Quantification of granzyme B mean fluorescence intensity (MFI) of stimulated iNKT cells and T_{CONV} normalized to isotype MFI indicated in bar graph. In all graphs, asterisks denote statistical significance (NS, non-significant; *p < 0.05, **p < 0.01, ***p < 0.001) determined by unpaired, two-way student's *t* tests in **(B, D)** and two-way analysis of variance (ANOVA) analysis in **(F)**. For all studies, biological replicates of human donor samples are indicated by symbols, and n=4 technical replicates were performed. Each biological replicate of matched donor cells was run in independent experiments.

indicates that unlike T_{CONV}, glutamine is not required for iNKT cell cytolytic protein production. Collectively, our data demonstrate that iNKT cells are able to maintain effector functions in both glutamine-deplete and glucose-deplete media conditions. These data suggest that within the nutrient-deplete conditions of the TME, iNKT cells might possess an ability to maintain certain anti-tumor effector functions relative to T_{CONV}, since T_{CONV} functional activity may be hampered due to their competition with tumor cells for glucose and glutamine.

Human iNKT Cells Display Enhanced Mitochondrial Metabolism and Fatty Acid Oxidation Relative to T_{CONV}

Memory T cells that develop after initial antigenic activation are primed for rapid reactivation upon secondary antigenic encounter. To allow for greater self-renewal capacity and longevity, memory T cells are metabolically adapted to possess altered mitochondrial morphology with enhanced spare respiratory capacity and a predominant reliance on oxidative and lipid metabolism (41, 42). We postulated that human iNKT cells may be "memory-like" in their metabolism. iNKT cells are poised for activation and express memory-like phenotypic markers, including CD62L, CCR7, and CD45RO (30, 43). Furthermore, murine NKT cells have been shown to depend on OXPHOS for survival, proliferation, and effector functions relative to CD4^{+} T cells (31). Collectively, it also appears that iNKT cells do not have a distinct differentiation hierarchy of naïve, effector, and memory states, further suggesting that their underlying metabolic program may be unique from T_{CONV}.
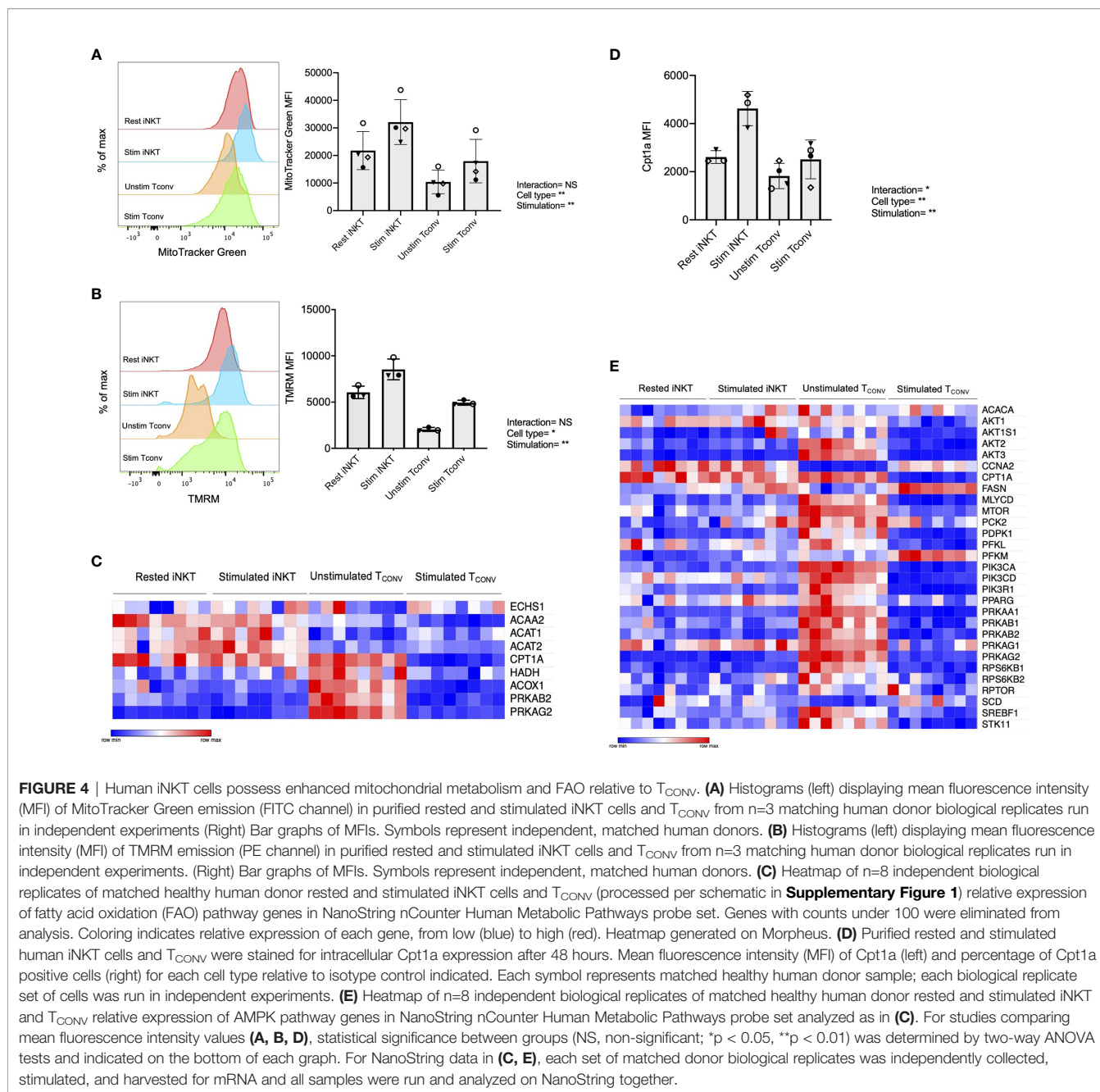
We first investigated mitochondrial parameters by flow cytometric dyes. Specifically, we utilized MitoTracker Green, which provides a measure of mitochondrial mass, as well as tetramethylrhodamine methyl ester perchlorate (TMRM), a cell permeable dye that accumulates in active mitochondria and serves as an indicator of mitochondrial membrane potential. We found that while both iNKT cells and T_{CONV} upregulate these parameters upon stimulation, iNKT cells have significantly higher mitochondrial mass (**Figure 4A**) and mitochondrial membrane potential (**Figure 4B**) relative to T_{CONV}. Together, this may imply greater mitochondrial activity within iNKT cells relative to T_{CONV}. Furthermore, NanoString transcriptional profiling of these cells revealed that resting and stimulated iNKT cells displayed significantly higher expression of several fatty acid oxidation (FAO) enzyme transcripts than stimulated T_{CONV} (**Figure 4C** and **Supplementary Table 2**). These genes include *Acaa2*, a mitochondrial enzyme involved in beta-oxidation of fatty acids into acetyl CoA, *Acat1* and *Acat2*, which convert ketones into acetyl-CoA, and *Acox1*, which also catalyzes beta-oxidation of fatty acids. One of the most striking differences was in the expression of *Cpt1a*, which encodes the rate-limiting enzyme of FAO that transports long-chain fatty acids into the mitochondria to be metabolized. Notably, *Cpt1a* was among the top 25 genes significantly higher in stimulated iNKT cells than stimulated T_{CONV}, underscoring the potential importance of this enzyme for human iNKT cells. Indeed, in support of this transcriptional data, we also find that iNKT cells

possess significantly higher levels of intracellular Cpt1a protein than T_{CONV} both at baseline and upon stimulation, as assessed by intracellular flow cytometry (**Figure 4D** and **Supplementary Figure 6**). These data suggest that iNKT cells may predominantly utilize FAO metabolism upon stimulation, which could represent a key metabolic difference from T_{CONV}.

In T_{CONV}, Cpt1a-mediated long-chain FAO supports the survival of memory T cells and regulatory T cells (29, 44). One master regulator that promotes FAO metabolism and memory cell differentiation is the nutrient sensor adenosine monophosphate-activated protein kinase (AMPK), which inhibits mTORC1 to promote catabolism and FAO, particularly in conditions of nutrient stress (44, 45). To further investigate whether iNKT cells displayed memory-like metabolism by employing FAO, we interrogated the expression of the 29 annotated genes in the NanoString AMPK signaling pathway probe set in human donor cell subsets. Intriguingly, of the 14 genes significantly differentially expressed between stimulated iNKT cells and T_{CONV}, 13 out of 14 were significantly higher in iNKT cells than stimulated T_{CONV} (**Figure 4E**). This further supports an important and distinct role for FAO metabolism in human iNKT cells relative to T_{CONV}.

Stimulated Human iNKT Cells Oxidize Fatty Acids to a Greater Extent Than Stimulated T_{CONV}

Given the striking differences in the expression of *Cpt1a* and other FAO genes between stimulated human iNKT cells and T_{CONV}, we postulated that these cells may differ in their use of FAO metabolism. To investigate the dependence on FAO for the metabolic activity of iNKT cells and T_{CONV} upon stimulation, we performed Seahorse extracellular flux analysis to generate real-time metabolic measurements of these cells. To specifically determine the contribution of fatty acids to the oxygen consumption rate (OCR) of stimulated iNKT cells and T_{CONV}, we injected into the cells either media only (vehicle) or etomoxir, a pharmacological inhibitor of Cpt1a. Upon etomoxir treatment, long-chain fatty acid import into the mitochondria is blocked, such that cytosolic fatty acids cannot be oxidized *via* the TCA cycle to fuel OXPHOS. Interestingly, we found that upon addition of carbonyl cyanide-4 (trifluoromethoxy) phenylhydrazone (FCCP) – which decouples the mitochondrial membrane to drive maximal substrate demand – etomoxir-treated iNKT cells displayed significantly reduced maximal respiration (**Figures 5A, C**). This indicates that fatty acids represent an important substrate for oxidation in stimulated iNKT cells. In contrast, stimulated T_{CONV} maintained equal levels of OCR upon FAO inhibition (**Figures 5B, C**), implying that in these cells, fatty acids do not represent a substrate for oxidation. In addition, we also quantified mitochondrial respiration-linked ATP production, defined as the difference in OCR at baseline and upon injection of oligomycin A, an ATP synthase inhibitor. Notably, this parameter was also significantly lowered in etomoxir-treated iNKT cells, but not in T_{CONV} (**Figure 5D**), further supporting the importance of FAO for contributing to ATP production derived from mitochondrial respiration in stimulated iNKT cells. Interestingly, depletion of fatty acids did not completely ablate OCR activity of iNKT cells, as they still displayed heightened

FIGURE 4 | Human iNKT cells possess enhanced mitochondrial metabolism and FAO relative to T_{CONV}. **(A)** Histograms (left) displaying mean fluorescence intensity (MFI) of MitoTracker Green emission (FITC channel) in purified rested and stimulated iNKT cells and T_{CONV} from n=3 matching human donor biological replicates run in independent experiments (Right) Bar graphs of MFIs. Symbols represent independent, matched human donors. **(B)** Histograms (left) displaying mean fluorescence intensity (MFI) of TMRM emission (PE channel) in purified rested and stimulated iNKT cells and T_{CONV} from n=3 matching human donor biological replicates run in independent experiments. (Right) Bar graphs of MFIs. Symbols represent independent, matched human donors. **(C)** Heatmap of n=8 independent biological replicates of matched healthy human donor rested and stimulated iNKT cells and T_{CONV} (processed per schematic in **Supplementary Figure 1**) relative expression of fatty acid oxidation (FAO) pathway genes in NanoString nCounter Human Metabolic Pathways probe set. Genes with counts under 100 were eliminated from analysis. Coloring indicates relative expression of each gene, from low (blue) to high (red). Heatmap generated on Morpheus. **(D)** Purified rested and stimulated human iNKT cells and T_{CONV} were stained for intracellular Cpt1a expression after 48 hours. Mean fluorescence intensity (MFI) of Cpt1a (left) and percentage of Cpt1a positive cells (right) for each cell type relative to isotype control indicated. Each symbol represents matched healthy human donor sample; each biological replicate set of cells was run in independent experiments. **(E)** Heatmap of n=8 independent biological replicates of matched healthy human donor rested and stimulated iNKT and T_{CONV} relative expression of AMPK pathway genes in NanoString nCounter Human Metabolic Pathways probe set analyzed as in **(C)**. For studies comparing mean fluorescence intensity values **(A, B, D)**, statistical significance between groups (NS, non-significant; *p < 0.05, **p < 0.01) was determined by two-way ANOVA tests and indicated on the bottom of each graph. For NanoString data in **(C, E)**, each set of matched donor biological replicates was independently collected, stimulated, and harvested for mRNA and all samples were run and analyzed on NanoString together.
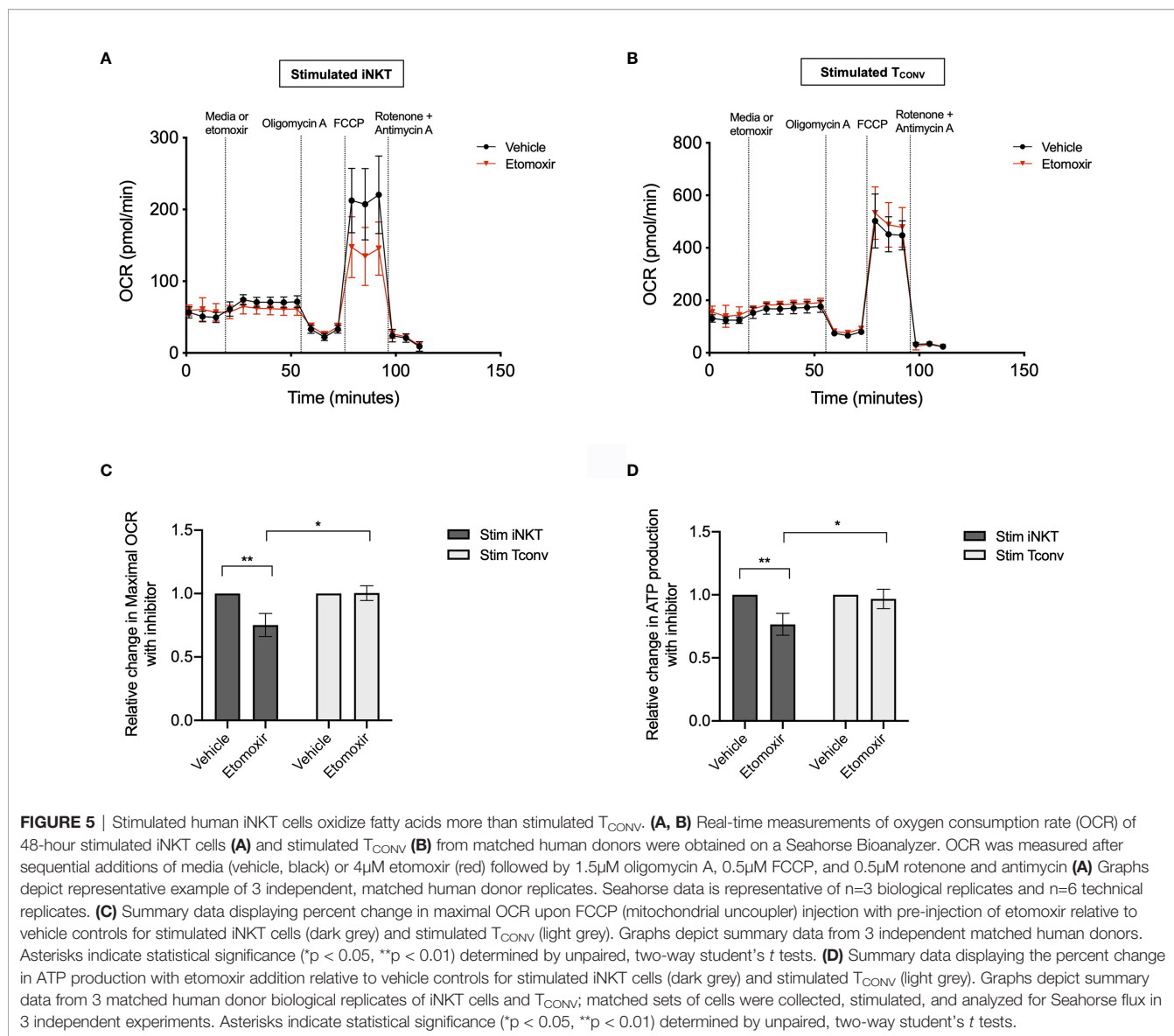
respiration upon addition of FCCP above basal OCR levels. This may suggest that iNKT cells do not solely depend on fatty acids and employ additional metabolic substrates for energy consumption upon stimulation. Nevertheless, our findings ultimately reveal a key bioenergetic difference between stimulated human iNKT cells and T_{CONV}, whereby in stimulated iNKT cells, fatty acids serve as a substrate contributing to fueling the TCA cycle and OXPHOS, while T_{CONV} preferentially rely on other substrates for oxidative metabolism, such as glucose and glutamine.

Taken together, our data reveals that human iNKT cells possess a unique metabolic profile from T_{CONV}, characterized by greater FAO metabolism and a reduced requirement for

glucose and glutamine for effector functions upon activation. Importantly, these differential bioenergetic requirements may allow iNKT cells to retain their functional activity in the nutrient-poor solid TME, where they may possess an advantage in competing with tumor cells relative to T_{CONV} that could potentially be exploited therapeutically.

DISCUSSION

One of the major limitations of iNKT-cell based immunotherapies is the lack of understanding of the cellular

FIGURE 5 | Stimulated human iNKT cells oxidize fatty acids more than stimulated T_{CONV}. **(A, B)** Real-time measurements of oxygen consumption rate (OCR) of 48-hour stimulated iNKT cells **(A)** and stimulated T_{CONV} **(B)** from matched human donors were obtained on a Seahorse Bioanalyzer. OCR was measured after sequential additions of media (vehicle, black) or 4μM etomoxir (red) followed by 1.5μM oligomycin A, 0.5μM FCCP, and 0.5μM rotenone and antimycin **(A)** Graphs depict representative example of 3 independent, matched human donor replicates. Seahorse data is representative of n=3 biological replicates and n=6 technical replicates. **(C)** Summary data displaying percent change in maximal OCR upon FCCP (mitochondrial uncoupler) injection with pre-injection of etomoxir relative to vehicle controls for stimulated iNKT cells (dark grey) and stimulated T_{CONV} (light grey). Graphs depict summary data from 3 independent matched human donors. Asterisks indicate statistical significance (*p < 0.05, **p < 0.01) determined by unpaired, two-way student's t tests. **(D)** Summary data displaying the percent change in ATP production with etomoxir addition relative to vehicle controls for stimulated iNKT cells (dark grey) and stimulated T_{CONV} (light grey). Graphs depict summary data from 3 matched human donor biological replicates of iNKT cells and T_{CONV}; matched sets of cells were collected, stimulated, and analyzed for Seahorse flux in 3 independent experiments. Asterisks indicate statistical significance (*p < 0.05, **p < 0.01) determined by unpaired, two-way student's t tests.

properties enabling long-term persistence within the TME. While new insights have begun to highlight the importance of cellular metabolism for sustained effector function and persistence of effector T cells within the TME, these insights have not been extended to iNKT cells – particularly human iNKT cells. To address this gap in knowledge, we sought to delineate the bioenergetic requirements of human iNKT cells relative to their conventional T cell counterparts. In the present study, we demonstrate for the first time that primary human PBMC-derived iNKT cells possess distinct metabolic features from matched T_{CONV} at both baseline and upon stimulation, and that these could potentially impact effector functions such as cytokine production and cytolysis. Specifically, we find that iNKT cells do not depend on glucose and glutamine for cytokine production and maintenance of granzyme B levels, and rather possess a "memory-like" metabolic phenotype

characterized by high mitochondrial mass and fatty acid oxidation metabolism. Notably, this represents a novel distinction in the link between metabolic and function in human iNKT cells relative to T_{CONV}; specifically, while memory T cells shift to glycolytic metabolism as they reprogram into effector cells, iNKT cells upon stimulation maintained high fatty acid and mitochondrial metabolism. While previous studies have begun to elucidate the immunometabolism of murine iNKT cells, these have utilized different methodologies, time points, and parameters by which to link metabolism to effector functions and have thus yielded different interpretations of how iNKT immunometabolism compares to that of T_{CONV}. On the one hand, in some contexts, iNKT cells appear to acutely utilize glycolysis immediately upon TCR stimulation (46), while on the other hand, others have found that these cells primarily depend upon

OXPHOS metabolism (31) and lipid biosynthesis (32). Moreover, the link between metabolism and effector functions is even less clear for human iNKT cells, emphasizing the need to characterize these properties.

lAlthough we observe key bioenergetic differences between human iNKT cells and T_{CONV} for stimulation-induced effector functions, we recognize that there are limitations and caveats to our present study that warrant further future studies of human iNKT cell immunometabolism. Firstly, due to technical limitations in obtaining sufficient cell numbers, we were unable to metabolically profile primary iNKT cells directly ex vivo from human donors and instead had to expand iNKT cell populations in culture. It is thus possible that the metabolic and functional features of these cells were altered during this expansion. To control for this to the best of our ability, we rested the iNKT cells post-expansion, prior to stimulating these side-by-side with matched, human donor-derived T_{CONV} under identical conditions. In future studies, single-cell approaches to investigating metabolism may corroborate and/or extend our findings regarding human iNKT cell immunometabolism. Secondly, based on the differences we observed between iNKT cell and T_{CONV} effector functions under TME-like conditions (glucose- and glutamine-depleted culture), we hypothesize similar outcomes within the TME. However, it is possible that iNKT cell metabolism varies in different peripheral tissues – and particularly within the TME - where infiltrating lymphocytes face nutrient competition with tumor cells, stromal cells, and immunosuppressive cells. To better understand the translational significance of iNKT cell immunometabolic properties and rationally design iNKT cell-based solid tumor immunotherapies, future studies aimed at delineating the metabolic and functional profiles of intratumoral iNKT cells and T_{CONV} relative to corresponding peripheral cells would be of great interest. Despite these caveats, we believe that that the novel bioenergetic differences we observed may distinguish iNKT cells from T_{CONV} in their ability to adapt, survive, and function in nutrient-poor conditions. Indeed, should future studies corroborate our hypothesis that iNKT cells possess the ability to retain effector functions and adapt to the nutrient-poor conditions of the solid tumor TME, this could have important implications for the use of iNKT cells in cancer immunotherapy.

The TME imposes metabolic challenges to the functions of T cells and other immune cells that directly impact antitumor immunity and tumor progression. As cancer and myeloid cells employ aerobic glycolysis to support biosynthetic requirements for proliferation *via* the Warburg effect, they rapidly uptake glucose, glutamine, and amino acids, depleting the TME of these nutrients (47–50); furthermore, the poor vasculature creates regions of hypoxia within the TME. As such, the hypoxic, acidic, nutrient-deplete TME impairs the ability of T_{CONV} to sustain their functional activity. Indeed, it is well appreciated that the ability of T_{CONV} to engage memory-like FAO metabolism results in improved persistence and anti-tumor activity within the TME (reviewed in (51). As such, the design of metabolic interventions to improve the efficacy of solid tumor immunotherapies provide an attractive therapeutic strategy. However, due to the metabolic similarities between tumor cells and effector T_{CONV} (52),

preserving anti-tumor immune cell function while specifically targeting tumor cell metabolism is difficult. Our observations, however, imply that the distinct bioenergetic requirements employed by iNKT cells may allow for the utility of metabolic modulators to specifically target tumor cells and their supportive myeloid cells without profoundly affecting iNKT cell effector functions. Specifically, we found that stimulated iNKT cells retain effector functions despite glucose and glutamine depletion; furthermore, unlike T_{CONV}, the effector mechanisms of iNKT cells appear to be decoupled from Myc signaling. Since Myc is an oncogenic driver in many cancers, targeting its activity is a key therapeutic strategy for attenuation of tumor cell growth. While such strategies would also significantly inhibit T_{CONV} activation (38), iNKT cell activity may be less affected, supporting the notion that adjunctive therapies that both boost iNKT cell function and inhibit tumor metabolism could be therapeutically valuable. Similarly, the use of inhibitors of glucose and glutamine metabolism may effectively target the bioenergetics of tumor cells and tumor-supportive myeloid cells while allowing for sustained iNKT cell effector functions. Thus, the unique metabolic features of iNKT cells may enable the use of broader metabolic interventions to which T_{CONV} may be particularly sensitive.

Interestingly, we observed that iNKT cells displayed higher expression of AMPK signaling genes relative to T_{CONV}. AMPK is a nutrient sensor that inhibits mTORC1 to promote catabolism and mitochondrial metabolism, including FAO (44, 45). Importantly, AMPK pathway activity has been shown to promote T cell longevity and survival, antigen recall responses in memory T cells (53, 54), and additionally promote T_{REG} differentiation and function (29). Our data suggests that like memory T cells and T_{REG} (as well as additional immunosuppressive populations, such as tumor-associated macrophages and myeloid-derived suppressor cells), the upregulation of AMPK-mediated catabolic metabolic programs may allow iNKT cells to adapt to the nutrient-deplete conditions of the TME. This presents a clear distinction from effector T_{CONV}, which depend upon anabolic metabolic pathways to sustain anti-tumor functions. In T_{REG}, the Forkhead Box protein (Foxp3) inhibits Myc signaling and glycolysis to promote OXPHOS and allow enhanced function in low-glucose, lactate-rich environments (55). Although lactic acid has previously been shown to blunt the effector functions of T and NK cells (56), as well as murine iNKT cells *in vitro* (57), a further dissection of its contribution to human iNKT cells and a better understanding of the metabolic flexibility of iNKT cells in acidic TME environments is important. Intriguingly, a recent study demonstrated that intratumoral T_{REG}, relative to peripheral T_{REG}, require the uptake of lactate – secreted by tumor cells – to maintain their suppressive effector functions within the TME (58). It is thus possible that human iNKT cells, given their overlapping metabolic profile with T_{REG}, could utilize similar mechanisms by which to employ metabolic flexibility in adapting to the acidic, nutrient-deplete TME. Given the link between *ex vivo* expansion and *in vivo* persistence of T_{CONV} within solid tumors (51), a greater understanding of the properties that would allow long-term persistence of exogenously expanded iNKT cells upon adoptive

transfer is desired. Nevertheless, our data suggest that at least some proportion of human PBMC-derived iNKT cells are memory-like in metabolism and may thus prove to be persistent within the TME.

Despite being in its early clinical stages, iNKT cell-based immunotherapies have begun to demonstrate some promise for solid tumors. One approach in phase I and II trials is the direct, adoptive transfer of activated iNKT cells, which has been tested in non-small cell lung cancer (59), head and neck squamous cell carcinoma [HNSCC; (17)]; and melanoma (19); these studies have demonstrated a transient boost in the numbers of circulating iNKT cells in patients and moderate stabilization of disease progression. Another approach currently under clinical investigation is the use of chimeric antigen receptor (CAR)-enabled iNKT cells. CAR-iNKT cells directed towards GD2, a disialoganglioside highly expressed on malignant neuroblastoma cells, are currently in phase I trials and preliminary studies indicate that the adoptively transferred iNKT cells localize to the tumor site and mediate tumor regression (20, 60).

A remaining challenge for the adoptive transfer strategies using iNKT cells is the ability to effectively expand sufficient numbers of cells *ex vivo*, given the low starting frequencies in peripheral blood. Recently, Zhu et al. demonstrated the preclinical feasibility and efficacy of hematopoietic stem cell (HSC)-derived iNKT cells to induce anti-tumor cytotoxicity in both hematologic and solid tumor models (61). This may allow for greater scalability and broader utility of iNKT-cell based immunotherapies. Additionally, given that iNKT cells are stimulated by monomorphic CD1d, it is formally possible to explore the use of allogeneic off-the-shelf iNKT cell products in hosts with severe immunocompromise who lack endogenous T cells and are incapable of host *vs.* graft responses. Interestingly, two studies of both *ex vivo*-expanded iNKT cells and CAR-iNKT cells have demonstrated that the most persistent effector populations – that retain anti-tumor function and maintain longevity within the TME – are those that express CD62L (62) and are transduced with IL-15 (63). Notably, in T_{CONV}, IL-15 promotes a more memory-like metabolic profile (41), and CD62L is also a central memory marker that is correlated with stem-like properties and enhanced anti-tumor efficacy (64–66); together, this further supports the link between iNKT cell metabolism and persistence in a tumor context. Overall, while iNKT cell-based immunotherapy platforms have demonstrated some early promise, ultimately, the long-term persistence and clinical efficacy remains unknown. However, the optimization of these strategies with additional knowledge gained from studies of iNKT cell metabolism would be of great value.

The present study is the first to characterize primary human iNKT cell metabolism side-by-side with T_{CONV}, and interestingly, reveals bioenergetic and functional differences between these lymphocyte populations that may bear important future clinical impact. Importantly, while our results suggest that iNKT cells may be more facile at adapting to the TME, they also prompt the need for metabolic characterization of iNKT cell subsets at baseline and upon stimulation directly from within the TME.

DATA AVAILABILITY STATEMENT

The raw data supporting the conclusions of this article will be made available by the authors, without undue reservation.

AUTHOR CONTRIBUTIONS

FUNDING

ACKNOWLEDGMENTS

SUPPLEMENTARY MATERIAL

The Supplementary Material for this article can be found online at: https://www.frontiersin.org/articles/10.3389/fimmu.2021.700374/full#supplementary-material

REFERENCES

1. Bendelac A, Savage PB, Teyton L. The Biology of NKT Cells. *Annu Rev Immunol* (2007) 25:297–336. doi: 10.1146/annurev.immunol.25.022106.141711

2. Brennan PJ, Brigl M, Brenner MB. Invariant Natural Killer T Cells: An Innate Activation Scheme Linked to Diverse Effector Functions. *Nat Rev Immunol* (2013) 13:101–17. doi: 10.1038/nri3369

3. Matsuda JL, Mallevaey T, Scott-Browne J, Gapin L. CD1d-Restricted Inkt Cells, the 'Swiss-Army Knife' of the Immune System. *Curr Opin Immunol* (2008) 20:358–68. doi: 10.1016/j.coi.2008.03.018

4. Wolf BJ, Choi JE, Exley MA. Novel Approaches to Exploiting Invariant NKT Cells in Cancer Immunotherapy. *Front Immunol* (2018) 9:384. doi: 10.3389/fimmu.2018.00384

5. Altman JB, Benavides AD, Das R, Bassiri H. Antitumor Responses of Invariant Natural Killer T Cells. *J Immunol Res* (2015) 2015:652875. doi: 10.1155/2015/652875

6. Kawano T, Cui J, Koezuka Y, Toura I, Kaneko Y, Motoki K, et al. CD1d-Restricted and TCR-Mediated Activation of V_α 14 NKT Cells by Glycosylceramides. *Science* (1997) 278:1626–9. doi: 10.1126/science.278.5343.1626

7. Bassiri H, Das R, Guan P, Barrett DM, Brennan PJ, Banerjee PP, et al. Inkt Cell Cytotoxic Responses Control T-Lymphoma Growth *In Vitro* and *In Vivo*. *Cancer Immunol Res* (2014) 2:59–69. doi: 10.1158/2326-6066.CIR-13-0104

8. Metelitsa LS, Naidenko OV, Kant A, Wu H-W, Loza MJ, Perussia B, et al. Human NKT Cells Mediate Antitumor Cytotoxicity Directly by Recognizing Target Cell CD1d With Bound Ligand or Indirectly by Producing IL-2 to Activate NK Cells. *J Immunol* (2001) 167:3114–22. doi: 10.4049/jimmunol.167.6.3114

9. Carnaud C, Lee D, Donnars O, Park S-H, Beavis A, Koezuka Y, et al. Cutting Edge: Cross-Talk Between Cells of the Innate Immune System: NKT Cells Rapidly Activate NK Cells. *J Immunol* (1999) 163:4647–50.

10. Mise N, Takami M, Suzuki A, Kamata T, Harada K, Hishiki T, et al. Antibody-Dependent Cellular Cytotoxicity Toward Neuroblastoma Enhanced by Activated Invariant Natural Killer T Cells. *Cancer Sci* (2016) 107:233–41. doi: 10.1111/cas.12882

11. Iyoda T, Yamasaki S, Hidaka M, Kawano F, Abe Y, Suzuki K, et al. Amelioration of NK Cell Function Driven by Vα24 + Invariant NKT Cell Activation in Multiple Myeloma. *Clin Immunol* (2018) 187:76–84. doi: 10.1016/j.clim.2017.10.007

12. Crowe NY, Smyth MJ, Godfrey DI. a Critical Role for Natural Killer T Cells in Immunosurveillance of Methylcholanthrene-Induced Sarcomas. *J Exp Med* (2002) 196:119–27. doi: 10.1084/jem.20020092

13. Smyth MJ, Crowe NY, Pellicci DG, Kyparissoudis K, Kelly JM, Takeda K, et al. Sequential Production of Interferon-Γ by NK1.1+ T Cells and Natural Killer Cells Is Essential for the Antimetastatic Effect of A-Galactosylceramide. *Blood* (2002) 99:1259–66. doi: 10.1182/blood.V99.4.1259

14. Kitamura H, Iwakabe K, Yahata T, Nishimura S, Ohta A, Ohmi Y, et al. The Natural Killer T (NKT) Cell Ligand Alpha-Galactosylceramide Demonstrates Its Immunopotentiating Effect by Inducing Interleukin (IL)-12 Production by Dendritic Cells and IL-12 Receptor Expression on NKT Cells. *J Exp Med* (1999) 189:1121–8. doi: 10.1084/jem.189.7.1121

15. Song L, Asgharzadeh S, Salo J, Engell K, Wu H, Sposto R, et al. Vα24-Invariant NKT Cells Mediate Antitumor Activity *via* Killing of Tumor-Associated Macrophages. *J Clin Invest* (2009) 119:1524–36. doi: 10.1172/JCI37869

16. Mussai F, De Santo C, Cerundolo V. Interaction Between Invariant NKT Cells and Myeloid-Derived Suppressor Cells in Cancer Patients: Evidence and Therapeutic Opportunities. *J Immunother* (2012) 35:449–59. doi: 10.1097/CJI.0b013e31825be926

17. Kunii N, Horiguchi S, Motohashi S, Yamamoto H, Ueno N, Yamamoto S, et al. Combination Therapy of *In Vitro*-Expanded Natural Killer T Cells and A-Galactosylceramide-Pulsed Antigen-Presenting Cells in Patients With Recurrent Head and Neck Carcinoma. *Cancer Sci* (2009) 100:1092–8. doi: 10.1111/j.1349-7006.2009.01135.x

18. Yamasaki K, Horiguchi S, Kurosaki M, Kunii N, Nagato K, Hanaoka H, et al. Induction of NKT Cell-Specific Immune Responses in Cancer Tissues After NKT Cell-Targeted Adoptive Immunotherapy. *Clin Immunol* (2011) 138:255–65. doi: 10.1016/j.clim.2010.11.014

19. Exley MA, Friedlander P, Alatrakchi N, Vriend L, Yue S, Sasada T, et al. Adoptive Transfer of Invariant NKT Cells as Immunotherapy for Advanced Melanoma: A Phase I Clinical Trial. *Clin Cancer Res* (2017) 23:3510–9. doi: 10.1158/1078-0432.CCR-16-0600

20. Heczey A, Liu D, Tian G, Courtney AN, Wei J, Marinova E, et al. Invariant NKT Cells With Chimeric Antigen Receptor Provide a Novel Platform for Safe and Effective Cancer Immunotherapy. *Blood* (2014) 124:2824–33. doi: 10.1182/blood-2013-11-541235

21. Rotolo A, Caputo VS, Holubova M, Baxan N, Dubois O, Chaudhry MS, et al. Enhanced Anti-Lymphoma Activity of CAR19-Inkt Cells Underpinned by Dual CD19 and CD1d Targeting. *Cancer Cell* (2018) 34:596–610.e11. doi: 10.1016/j.ccell.2018.08.017

22. Pearce EL, Poffenberger MC, Chang C-H, Jones RG. Fueling Immunity: Insights Into Metabolism and Lymphocyte Function. *Science* (2013) 342:1242454. doi: 10.1126/science.1242454

23. Gubser PM, Bantug GR, Razik L, Fischer M, Dimeloe S, Hoenger G, et al. Rapid Effector Function of Memory CD8+ T Cells Requires an Immediate-Early Glycolytic Switch. *Nat Immunol* (2013) 14:1064–72. doi: 10.1038/ni.2687

24. Chang C-H, Qiu J, O'Sullivan D, Buck MD, Noguchi T, Curtis JD, et al. Metabolic Competition In the Tumor Microenvironment Is a Driver of Cancer Progression. *Cell* (2015) 162:1229–41. doi: 10.1016/j.cell.2015.08.016

25. Ho P-C, Bihuniak JD, Macintyre AN, Staron M, Liu X, Amezquita R, et al. Phosphoenolpyruvate Is a Metabolic Checkpoint of Anti-Tumor T Cell Responses. *Cell* (2015) 162:1217–28. doi: 10.1016/j.cell.2015.08.012

26. Buck MD, O'Sullivan D, Klein Geltink RI, Curtis JD, Chang C-H, Sanin DE, et al. Mitochondrial Dynamics Controls T Cell Fate Through Metabolic Programming. *Cell* (2016) 166:63–76. doi: 10.1016/j.cell.2016.05.035

27. Scharping NE, Menk AV, Moreci RS, Whetstone RD, Dadey RE, Watkins SC, et al. The Tumor Microenvironment Represses T Cell Mitochondrial Biogenesis to Drive Intratumoral T Cell Metabolic Insufficiency and Dysfunction. *Immunity* (2016) 45:374–88. doi: 10.1016/j.immuni.2016.07.009

28. Sukumar M, Liu J, Ji Y, Subramanian M, Crompton JG, Yu Z, et al. Inhibiting Glycolytic Metabolism Enhances CD8+ T Cell Memory and Antitumor Function. *J Clin Invest* (2013) 123:4479–88. doi: 10.1172/JCI69589

29. Michalek RD, Gerriets VA, Jacobs SR, Macintyre AN, MacIver NJ, Mason EF, et al. Cutting Edge: Distinct Glycolytic and Lipid Oxidative Metabolic Programs Are Essential for Effector and Regulatory CD4 $^+$ T Cell Subsets. *J Immunol* (2011) 186:3299–303. doi: 10.4049/jimmunol.1003613

30. D'Andrea A, Goux D, Lalla CD, Koezuka Y, Montagna D, Moretta A, et al. Neonatal Invariant Vα24+ NKT Lymphocytes Are Activated Memory Cells. *Eur J Immunol* (2000) 30:1544–50. doi: 10.1002/1521-4141(200006)30:6<1544::AID-IMMU1544>3.0.CO;2-I

31. Kumar A, Pyaram K, Yarosz EL, Hong H, Lyssiotis CA, Giri S, et al. Enhanced Oxidative Phosphorylation in NKT Cells Is Essential for Their Survival and Function. *Proc Natl Acad Sci USA* (2019) 116:7439–48. doi: 10.1073/pnas.1901376116

32. Fu S, He K, Tian C, Sun H, Zhu C, Bai S, et al. Impaired Lipid Biosynthesis Hinders Anti-Tumor Efficacy of Intratumoral Inkt Cells. *Nat Commun* (2020) 11:438. doi: 10.1038/s41467-020-14332-x

33. Cham CM, Gajewski TF. Glucose Availability Regulates IFN-Gamma Production and P70s6 Kinase Activation in CD8+ Effector T Cells. *J Immunol* (2005) 174:4670–7. doi: 10.4049/jimmunol.174.8.4670

34. Cham CM, Driessens G, O'Keefe JP, Gajewski TF. Glucose Deprivation Inhibits Multiple Key Gene Expression Events and Effector Functions in CD8+ T Cells. *Eur J Immunol* (2008) 38:2438–50. doi: 10.1002/eji.200838289

35. Chang C-H, Curtis JD, Maggi LB, Faubert B, Villarino AV, O'Sullivan D, et al. Posttranscriptional Control of T Cell Effector Function by Aerobic Glycolysis. *Cell* (2013) 153:1239–51. doi: 10.1016/j.cell.2013.05.016

36. Bengsch B, Johnson AL, Kurachi M, Odorizzi PM, Pauken KE, Attanasio J, et al. Bioenergetic Insufficiencies Due to Metabolic Alterations Regulated by the Inhibitory Receptor PD-1 Are an Early Driver of CD8(+) T Cell Exhaustion. *Immunity* (2016) 45:358–73. doi: 10.1016/j.immuni.2016.07.008

37. Pajak B, Siwiak E, Sołtyka M, Priebe A, Zieliński R, Fokt I, et al. 2-Deoxy-D-Glucose and Its Analogs: From Diagnostic to Therapeutic Agents. *Int J Mol Sci* (2020) 21:234. doi: 10.3390/ijms21010234

38. Wang R, Dillon CP, Shi LZ, Milasta S, Carter R, Finkelstein D, et al. The Transcription Factor Myc Controls Metabolic Reprogramming Upon T Lymphocyte Activation. *Immunity* (2011) 35:871–82. doi: 10.1016/j.immuni.2011.09.021

39. Carr EL, Kelman A, Wu GS, Gopaul R, Senkevitch E, Aghvanyan A, et al. Glutamine Uptake and Metabolism Are Coordinately Regulated by ERK/MAPK During T Lymphocyte Activation. *J Immunol* (2010) 185:1037–44. doi: 10.4049/jimmunol.0903586

40. Nakaya M, Xiao Y, Zhou X, Chang J-H, Chang M, Cheng X, et al. Inflammatory T Cell Responses Rely on Amino Acid Transporter ASCT2 Facilitation of Glutamine Uptake and mTORC1 Kinase Activation. *Immunity* (2014) 40:692–705. doi: 10.1016/j.immuni.2014.04.007

41. van der Windt G, Everts B, Chang C-H, Curtis JD, Freitas TC, Amiel E, et al. Mitochondrial Respiratory Capacity Is a Critical Regulator of CD8+ T Cell Memory Development. *Immunity* (2012) 36:68–78. doi: 10.1016/j.immuni.2011.12.007

42. van der Windt GJW, O'Sullivan D, Everts B, Huang SC-C, Buck MD, Curtis JD, et al. CD8 Memory T Cells Have a Bioenergetic Advantage That Underlies Their Rapid Recall Ability. *Proc Natl Acad Sci* (2013) 110:14336–41. doi: 10.1073/pnas.1221740110

43. Baev DV, Peng X, Song L, Barnhart JR, Crooks GM, Weinberg KI, et al. Distinct Homeostatic Requirements of CD4+ and CD4- Subsets of Vα24-Invariant Natural Killer T Cells in Humans. *Blood* (2004) 104:4150–6. doi: 10.1182/blood-2004-04-1629

44. Pearce EL, Walsh MC, Cejas PJ, Harms GM, Shen H, Wang L-S, et al. Enhancing CD8 T Cell Memory by Modulating Fatty Acid Metabolism. *Nature* (2009) 460:103–7. doi: 10.1038/nature08097

45. Rolf J, Zarrouk M, Finlay DK, Foretz M, Viollet B, Cantrell DA. AMPKα1: A Glucose Sensor That Controls CD8 T-Cell Memory. *Eur J Immunol* (2013) 43:889–96. doi: 10.1002/eji.201243008

46. Fu S, Zhu S, Tian C, Bai S, Zhang J, Zhan C, et al. Immunometabolism Regulates TCR Recycling and iNKT Cell Functions. *Sci Signal* (2019) 12: eaau1788. doi: 10.1126/scisignal.aau1788

47. DeBerardinis RJ, Chandel NS. Fundamentals of Cancer Metabolism. *Sci Adv* (2016) 2:e1600200. doi: 10.1126/sciadv.1600200

48. Pavlova NN, Thompson CB. The Emerging Hallmarks of Cancer Metabolism. *Cell Metab* (2016) 23:27–47. doi: 10.1016/j.cmet.2015.12.006

49. Ghoshdastider U, Rohatgi N, Mojtabavi Naeini M, Baruah P, Revkov E, Guo YA, et al. Pan-Cancer Analysis of Ligand-Receptor Crosstalk in the Tumor Microenvironment. *Cancer Res* (2021) 81:1802–12. doi: 10.1158/0008-5472.CAN-20-2352

50. Reinfeld BI, Madden MZ, Wolf MM, Chytil A, Bader JE, Patterson AR, et al. Cell-Programmed Nutrient Partitioning in the Tumour Microenvironment. *Nature* (2021) 593:282–8. doi: 10.1038/s41586-021-03442-1

51. Kishton RJ, Sukumar M, Restifo NP. Metabolic Regulation of T Cell Longevity and Function in Tumor Immunotherapy. *Cell Metab* (2017) 26:94–109. doi: 10.1016/j.cmet.2017.06.016

52. Allison KE, Coomber BL, Bridle BW. Metabolic Reprogramming in the Tumour Microenvironment: A Hallmark Shared by Cancer Cells and T Lymphocytes. *Immunology* (2017) 152:175–84. doi: 10.1111/imm.12777

53. Blagih J, Coulombe F, Vincent EE, Dupuy F, Galicia-Vázquez G, Yurchenko E, et al. The Energy Sensor AMPK Regulates T Cell Metabolic Adaptation and Effector Responses *In Vivo*. *Immunity* (2015) 42:41–54. doi: 10.1016/j.immuni.2014.12.030

54. Kishton RJ, Barnes CE, Nichols AG, Cohen S, Gerriets VA, Siska PJ, et al. AMPK Is Essential to Balance Glycolysis and Mitochondrial Metabolism to Control T-ALL Cell Stress and Survival. *Cell Metab* (2016) 23:649–62. doi: 10.1016/j.cmet.2016.03.008

55. Angelin A, Gil-de-Gómez L, Dahiya S, Jiao J, Guo L, Levine MH, et al. Foxp3 Reprograms T Cell Metabolism to Function in Low Glucose High Lactate Environments. *Cell Metab* (2017) 25:1282–1293.e7. doi: 10.1016/j.cmet.2016.12.018

56. Brand A, Singer K, Koehl GE, Kolitzus M, Schoenhammer G, Thiel A, et al. LDHA-Associated Lactic Acid Production Blunts Tumor Immunosurveillance by T and NK Cells. *Cell Metab* (2016) 24:657–71. doi: 10.1016/j.cmet.2016.08.011

57. Xie D, Zhu S, Bai L. Lactic Acid in Tumor Microenvironments Causes Dysfunction of NKT Cells by Interfering With mTOR Signaling. *Sci China Life Sci* (2016) 59:1290–6. doi: 10.1007/s11427-016-0348-7

58. Watson MJ, Vignali PDA, Mullett SJ, Overacre-Delgoffe AE, Peralta RM, Grebinoski S, et al. Metabolic Support of Tumour-Infiltrating Regulatory T Cells by Lactic Acid. *Nature* (2021) 591:645–51. doi: 10.1038/s41586-020-03045-2

59. Shin T, Nakayama T, Akutsu Y, Motohashi S, Shibata Y, Harada M, et al. Inhibition of Tumor Metastasis by Adoptive Transfer of IL-12-Activated Vα14 NKT Cells. *Int J Cancer* (2001) 91:523–8. doi: 10.1002/1097-0215(20010215)91:4<523::AID-IJC1087>3.0.CO;2-L

60. Heczey A, Courtney AN, Montalbano A, Robinson S, Liu K, Li M, et al. Anti-GD2 CAR-NKT Cells in Patients With Relapsed or Refractory Neuroblastoma: An Interim Analysis. *Nat Med* (2020) 26:1686–90. doi: 10.1038/s41591-020-1074-2

61. Zhu Y, Smith DJ, Zhou Y, Li Y-R, Yu J, Lee D, et al. Development of Hematopoietic Stem Cell-Engineered Invariant Natural Killer T Cell Therapy for Cancer. *Cell Stem Cell* (2019) 25:542–57.e9. doi: 10.1016/j.stem.2019.08.004

62. Tian G, Courtney AN, Jena B, Heczey A, Liu D, Marinova E, et al. CD62L+ NKT Cells Have Prolonged Persistence and Antitumor Activity *In Vivo*. *J Clin Invest* (2016) 126:2341–55. doi: 10.1172/JCI83476

63. Xu X, Huang W, Heczey A, Liu D, Guo L, Wood M, et al. NKT Cells Coexpressing a GD2-Specific Chimeric Antigen Receptor and IL15 Show Enhanced *In Vivo* Persistence and Antitumor Activity Against Neuroblastoma. *Clin Cancer Res* (2019) 25:7126–38. doi: 10.1158/1078-0432.CCR-19-0421

64. Graef P, Buchholz VR, Stemberger C, Flossdorf M, Henkel L, Schiemann M, et al. Serial Transfer of Single-Cell-Derived Immunocompetence Reveals Stemness of CD8(+) Central Memory T Cells. *Immunity* (2014) 41:116–26. doi: 10.1016/j.immuni.2014.05.018

65. Wang X, Naranjo A, Brown CE, Bautista C, Wong CW, Chang W-C, et al. Phenotypic and Functional Attributes of Lentivirus-Modified CD19-Specific Human CD8+ Central Memory T Cells Manufactured at Clinical Scale. *J Immunother* (2012) 35:689–701. doi: 10.1097/CJI.0b013e318270dec7

66. Sommermeyer D, Hudecek M, Kosasih PL, Gogishvili T, Maloney DG, Turtle CJ, et al. Chimeric Antigen Receptor-Modified T Cells Derived From Defined CD8+ and CD4+ Subsets Confer Superior Antitumor Reactivity *in Vivo*. *Leukemia* (2016) 30:492–500. doi: 10.1038/leu.2015.247